(46)

Measurement of the second-order nonlinear susceptibility of proton-exchanged $LiNbO_3$

M. L. Bortz and M. M. Fejer

Edward L. Ginzton Laboratory, Stanford University, Stanford, California 94305

Received December 24, 1991

We have measured the d_{33} nonlinear coefficient in proton-exchanged $LiNbO_3$ by using angle-dependent reflected second-harmonic generation and observed a reduction to ≤1% of the bulk $LiNbO_3$ value.

Proton exchange is an attractive technique for fabricating optical waveguides in $LiNbO_3$. The low temperature and high surface index change (≈0.125 at 633 nm) of the proton-exchange process increase the processing latitude and range of guided-wave devices that can be fabricated over those possible with high-temperature metal-indiffusion waveguide technologies. However, the r_{33} electro-optic coefficient in proton-exchanged $LiNbO_3$ (PE-$LiNbO_3$) has been measured to be between 5% (Ref. 1) and 10% (Ref. 2) of the bulk $LiNbO_3$ value. Postexchange low-temperature annealing ($T \approx 350$°C) restores the electro-optic coefficient to its bulk value,[3] and many electro-optic devices have been developed by using annealed PE-$LiNbO_3$ waveguides. The nonlinear susceptibility of $LiNbO_3$ also appears to be degraded by proton exchange. Recent attempts to measure directly the d_{33} nonlinear-optical coefficient in PE-$LiNbO_3$ have resulted in values between 0.5 (Ref. 4) and 0.63 (Ref. 5) of the bulk $LiNbO_3$ value, with partial restoration with annealing.[5] The magnitude of the nonlinear coefficient versus the index change plays an essential role in the design of efficient guided-wave nonlinear-optical devices. In this Letter we report measurements and theory of angle-dependent reflected second-harmonic generation (SHG) that show that d_{33} in PE-$LiNbO_3$ is ≤1% of the bulk $LiNbO_3$ value, in contradiction with previously reported measurements at optical frequencies.

PE-$LiNbO_3$ generally exists as only a thin layer on a $LiNbO_3$ substrate, so measurement of the nonlinear susceptibility of PE-$LiNbO_3$ by using conventional methods appropriate for bulk materials, such as the transmission Maker fringe or phase-matched SHG techniques, is impractical. To measure accurately the nonlinear susceptibility of a proton-exchanged layer on $LiNbO_3$, discrimination against nonlinear signals originating in the bulk $LiNbO_3$ substrate is necessary. Guided-wave quasi-phase-matched nonlinear interactions in PE-$LiNbO_3$ sample the proton-exchanged region but are sensitive only to the average value of d_{33} weighted by the modal fields and thus are difficult to analyze quantitatively. However, a SHG experiment performed in reflection would be sensitive to the surface PE-$LiNbO_3$ layer.

The analysis of second-harmonic (SH) fields present in reflection from materials with second-order nonlinear susceptibilities cannot be performed by using the slowly varying envelope approximation and requires a careful theoretical formulation.[6] As shown in Ref. 6, a single fundamental field at a frequency ω incident upon a material with a nonzero second-order nonlinear susceptibility generates a transmitted wave at 2ω composed of free and forced waves, which interfere in the crystal with a characteristic length termed the coherence length (l_c), and a reflected signal at 2ω that is necessary to satisfy the continuity of the tangential field components at the interface. The reflected field is generated at interfaces consisting of nonlinear susceptibility discontinuities, even in the absence of a refractive-index discontinuity associated with the interface. A fundamental field incident upon a nonlinear film on a nonlinear substrate generates a reflected SH field at the air–film and the film–substrate interfaces. These contributions combine interferometrically outside the multilayer structure, resulting in a reflected SH intensity that depends on the incident angle (θ^a), the film thickness (l), the refractive indices at ω and 2ω in the film ($n^f_\omega, n^f_{2\omega}$) and in the substrate ($n^s_\omega, n^s_{2\omega}$), and the nonlinear susceptibilities of the film [$\chi^{(2)f}$] and the substrate [$\chi^{(2)s}$]. An index discontinuity associated with the film–substrate interface will reflect a portion of the SH field generated in the film by the forward-propagating fundamental field, which will also contribute interferometrically to the reflected intensity. Enhancement of this field increases sensitivity to small film nonlinear susceptibilities, so choosing the film thickness such that $l = (2m - 1)l_c$ increases sensitivity over $l = 2ml_c$, where m is an integer. While the angular positions of the maxima and minima of the intensity fringes are dependent on the relative phase of the fields, the fringe amplitude is a strong function of the ratio $\chi^{(2)f}/\chi^{(2)s}$. Measurement of the reflected SH intensity versus the incident angle, along with a separate measurement of the film thickness and refractive indices, can be used to determine the ratio $\chi^{(2)f}/\chi^{(2)s}$.

Figure 1 illustrates the fields necessary to determine the magnitude of the reflected SH field from

0146-9592/92/100704-03$5.00/0

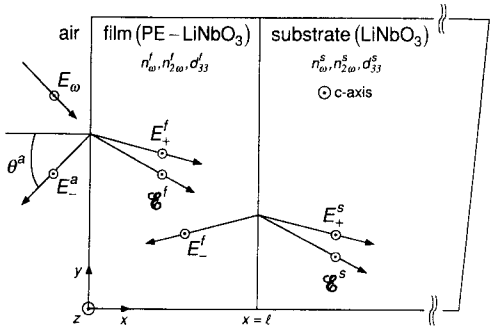

Fig. 1. Diagram of the interacting waves for calculation of the angle-dependent reflected SHG from a nonlinear film on a nonlinear substrate. The forced waves are $\mathscr{E}^f$ and $\mathscr{E}^s$, whereas the free waves are E_-^a, E_+^f, E_-^f, and E_+^s.

$PE\text{-}LiNbO_3$. Our analysis is based on that given in Ref. 6 for the reflected SH field from a homogeneous nonlinear material. The two-layer system considered here consists of a film and a semi-infinite substrate that have arbitrary linear and nonlinear susceptibilities. We simplify the calculation by assuming a one-dimensional geometry for the media and the fields, propagation in the x–y plane parallel to a principal axis of the dielectric tensor (e.g., perpendicular to the optical axis of a uniaxial crystal), and polarization along the z axis perpendicular to the plane of incidence for all the fields (TE polarization). With the c axis of the $LiNbO_3$ substrate aligned parallel to the z axis, the fundamental and SH fields are coupled by the d_{33} nonlinear coefficient of $PE\text{-}LiNbO_3$. We neglect the fundamental field reflection at the film–substrate interface, which is valid for small film–substrate refractive-index differences. On substitution into the wave equation the known nonlinear polarizations ($\mathbf{P}_{2\omega}^{f,s} = \epsilon_0 d_{33}^{f,s} \mathbf{E}_\omega \cdot \mathbf{E}_\omega$) yield the forced waves in the film [$\mathscr{E}^f \exp(i2\mathbf{k}_\omega^f \cdot \mathbf{r})$] and the substrate {$\mathscr{E}^s \exp[i2(\mathbf{k}_\omega^f - \mathbf{k}_\omega^s) \cdot (l\hat{x})]\exp(i2\mathbf{k}_\omega^s \cdot \mathbf{r})$}, where $|\mathbf{k}_\omega^{f,s}| = 2\pi n_\omega^{f,s}/\lambda_\omega$. The forced waves have amplitudes given by

$$\mathscr{E}^f = \frac{\hat{z} d_{33}^f (t_\omega^{af} E_\omega)^2}{(n_{2\omega}^f + n_\omega^f)(n_{2\omega}^f - n_\omega^f)}, \tag{1}$$

$$\mathscr{E}^s = \frac{\hat{z} d_{33}^f (t_\omega^{af} t_\omega^{fs} E_\omega)^2}{(n_{2\omega}^s + n_\omega^s)(n_{2\omega}^s - n_\omega^s)}, \tag{2}$$

where t_ω^{af} and t_ω^{fs} are the linear Fresnel transmission factors for the fundamental field at the air–film and film–substrate interfaces, respectively. The four unknown free 2ω fields polarized along z consist of the reflected wave in air [$\mathbf{E}_-^a \exp(i\mathbf{k}_-^a \cdot \mathbf{r})$], the forward-[$\mathbf{E}_+^f \exp(i\mathbf{k}_+^f \cdot \mathbf{r})$] and backward-[$\mathbf{E}_-^f \exp(i\mathbf{k}_-^f \cdot \mathbf{r})$] propagating free waves in the film, and the free wave ($\mathbf{E}_+^s \exp\{i\mathbf{k}_+^s \cdot [\mathbf{r} - (l\hat{x})]\}$) in the bulk, where $|\mathbf{k}_\pm^{a,f,s}| = 2\pi n_{2\omega}^{a,f,s}/\lambda_{2\omega}$. The angles of incidence, $\theta^{a,f,s}$ for the free waves and $\phi^{f,s}$ for the forced waves, can be derived from conservation of tangential wave vector at 2ω and are given in Ref. 6; these angles are not shown in Fig. 1 to improve visual clarity.

The boundary conditions at the two interfaces can be used to solve for the reflected field amplitude in terms of the known nonlinear polarizations. With the phase factors defined as $\beta^{a,f,s} = |\mathbf{k}_\pm^{a,f,s}| \cos\theta^{a,f,s}$ and $\Phi^{f,s} = 2|\mathbf{k}_\omega^{f,s}| \cos\phi^{f,s}$, the two equations derived from continuity of E_z and H_y at the air–film interface ($x = 0$) are

$$E_-^a = E_+^f + E_-^f + \mathscr{E}^f, \tag{3}$$

$$-\beta^a E_-^a = \beta^f E_+^f - \beta^f E_-^f + \Phi^f \mathscr{E}^f. \tag{4}$$

The two equations at the film–substrate interface ($x = l$) are

$$E_+^f \exp(i\beta^f l) + E_-^f \exp(-i\beta^f l) + \mathscr{E}^f \exp(i\Phi^f l) = E_+^s + \mathscr{E}^s \exp(i\Phi^f l), \tag{5}$$

$$\beta^f E_+^f \exp(i\beta^f l) - \beta^f E_-^f \exp(-i\beta^f l) + \Phi^f \mathscr{E}^f \exp(i\Phi^f l) = \beta^s E_+^s + \Phi^s \mathscr{E}^s \exp(i\Phi^f l). \tag{6}$$

The angular dependence of the reflected SH field (E_-^a) can be obtained by solving the system of linear equations as a function of θ^a. The reflected SH field from a nonlinear slab bounded on both sides by linear dielectric media can be obtained by setting $d_{33}^s = 0$, with the result given in Eqs. 6.7–6.9 in Ref. 6. The reflected SH field from a bulk medium is obtained by setting $n_\omega^f = n_\omega^s$, $n_{2\omega}^f = n_{2\omega}^s$, and $d_{33}^f = d_{33}^s$, as in Eq. 4.4 in Ref. 6.

To determine d_{33} of $PE\text{-}LiNbO_3$ we measured the reflected SH intensity as a function of the incident angle. An injection-seeded Q-switched Nd:YAG laser ($\lambda_\omega = 1.06\ \mu m$) was weakly focused ($f$-number ≈ 100) onto the sample, and the reflected SH field was detected with a photomultiplier tube with a GaAs photocathode and a gated integrator. The substrate orientation and field polarizations are shown in Fig. 1. Data were obtained for $20° < \theta^a < 60°$ in 5° increments from the $PE\text{-}LiNbO_3$ sample and an untreated $LiNbO_3$ reference. The back surface of the wafer was wedged at ≈2° to separate substrate SHG specularly reflected from the back surface of the wafer from the first surface reflection, and the former reflection was blocked with an aperture. The $PE\text{-}LiNbO_3$ samples were fabricated on x-cut $LiNbO_3$ by proton exchange in pure benzoic acid for 2 h at 220°C. IWKB analysis

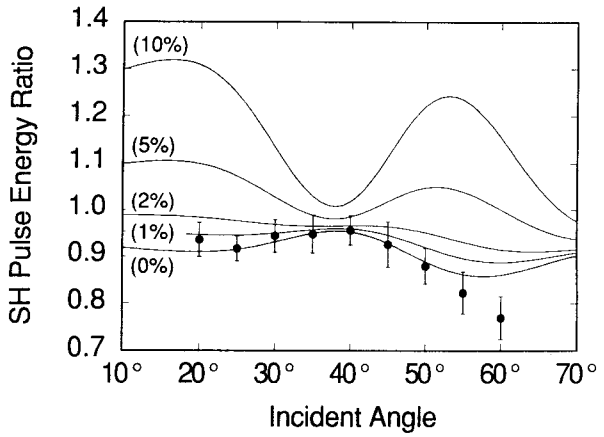

Fig. 2. SH pulse energy from $PE\text{-}LiNbO_3$ normalized to the SH pulse energy from bulk $LiNbO_3$. The curves are parameterized by d_{33}^f/d_{33}^s.

of the effective index data obtained by prism coupling at 458 nm yielded a steplike index profile with a thickness of 2.1 ± 0.1 μm. The surface extraordinary refractive-index change at 458 nm was 0.184, in good agreement with studies of the dispersion in PE-$LiNbO_3$.[7] For subsequent calculations the index changes that are due to proton exchange at λ_ω and $\lambda_{2\omega}$ were taken to be 0.1 and 0.15, respectively. With the bulk $LiNbO_3$ indices taken from the literature,[8] l_c in PE-$LiNbO_3$ for $\lambda_\omega = 1.06$ μm is 2.05 μm, which is extremely close to the film thickness.

The angular dependence of the reflected SH pulse energy from the untreated $LiNbO_3$ reference agreed well with the theoretical curve calculated from Eqs. (1)–(6). As expected, a decrease in SH pulse energy with increasing angle was observed, caused primarily by the reduced nonlinear polarization that was due to linear reflection of the fundamental field. Figure 2 shows the SH pulse energy from the PE-$LiNbO_3$ sample, normalized at each angle to the bulk $LiNbO_3$ data to emphasize the interference effects. The theoretical curves are parameterized by d_{33}^f/d_{33}^s and were calculated by using a film thickness of 2.08 μm, determined by treating the thickness as an adjustable parameter, within the range measured by prism coupling, in order to best fit the theory to the data. Since $l \approx l_c$, nonzero values of d_{33}^f result in a forward-propagating SH wave that is reflected from the film–substrate interface, which increases the theoretical reflected SH pulse energy above that of bulk $LiNbO_3$. Comparison between the data and theory shows that d_{33} in PE-$LiNbO_3$ is ≤1% of the value in bulk $LiNbO_3$.

One assumption in the above calculation, suggested by previous measurements of PE-$LiNbO_3$ waveguides that indicate step proton concentration and refractive-index profiles, is the existence of an abrupt film–substrate interface. This assumption was tested by attempting to fit the data presented in Fig. 2 to models based on a graded interface, detailed discussion of which is beyond the scope of this Letter. It was not possible to fit the data with any of these models, consistent with the assumption of an abrupt interface. A second assumption is the neglect of the fundamental field reflection at the film–substrate interface (2% in this case). The error in the calculated reflected SHG as a result of this effect is <4% when $d_{33}^f = 0$ and <8% when $d_{33}^f = d_{33}^s$. Neglect of the fundamental field reflection does not affect the results presented above but must be included if this technique is applied to systems with larger index differences.

A recent measurement[5] of d_{33} in PE-$LiNbO_3$ used angle-dependent reflection SHG and gave a value for d_{33} of 50% of the value in bulk $LiNbO_3$. We fabricated a PE-$LiNbO_3$ waveguide using identical conditions to those given in Ref. 5, and our measurements indicated that the d_{33} of this PE-$LiNbO_3$ layer was also ≤1% of the value in bulk $LiNbO_3$. However, the authors of Ref. 5 neglected the effect of the reflected SH intensity on both the d_{33} discontinuity at the film–substrate interface and the angular dependence of the nonlinear polarization [which scales as $(t_\omega^{af})^4$], which suggests that the difference between our results and those of Ref. 5 are due to analysis rather than processing conditions.

We cannot explain the disagreement between the results presented here and the first measurements[4] of d_{33} in PE-$LiNbO_3$, which used diffraction through a proton-exchanged grating to extract a value for d_{33} of 50% of the value in bulk $LiNbO_3$. However, we note that the theory used in Ref. 4 is sensitive to the linear properties of the grating, because changes such as surface index, waveguide depth, grating duty cycle, and shape of the proton-exchanged region affect the magnitude of the Fourier components of the grating. The coupling between the linear and nonlinear properties of the grating becomes even more complex with annealing, which makes accurate extraction of d_{33} difficult.

We have shown that the d_{33} nonlinear coefficient of PE-$LiNbO_3$ is ≤1% of the bulk $LiNbO_3$ value. The magnitude of the reduction is similar to that observed in the r_{33} electro-optic coefficient but is inconsistent with recent measurements of d_{33} in PE-$LiNbO_3$, which indicate a 50% reduction when compared with the value in bulk $LiNbO_3$. However, a vanishing d_{33} in PE-$LiNbO_3$ is consistent with our observations that the efficiency of quasi-phase-matched frequency doublers fabricated by using proton-exchanged waveguides are orders of magnitude smaller than those of similar devices fabricated with annealed-proton-exchanged waveguides. Even from the latter devices, observed normalized conversion efficiencies are significantly smaller than theoretical values,[9] which may be due to only a partial restoration of d_{33} with annealing. Measurements of d_{33} in annealed PE-$LiNbO_3$ waveguides are ongoing.

The authors acknowledge useful discussions with Eric Lim, Bob Eckardt, Dieter Jundt, and Eric Gustafson. This research was supported by the Defense Advanced Research Projects Agency, the Joint Services Electronics Program, and Crystal Technology, Inc.

Note added in proof: Laurell *et al.*[10] have recently reported similar results for d_{33} in PE-$LiNbO_3$.

References

1. Y. Kondo, L. Hu, and Y. Fujii, Trans. Inst. Electr. Inf. Commun. Eng. **E71,** 1122 (1988).
2. M. Minakata, K. Kumagai, and S. Kawakami, Appl. Phys. Lett. **49,** 992 (1986).
3. P. G. Suchoski, T. K. Findakly, and F. J. Leonberger, Opt. Lett. **13,** 1050 (1988).
4. T. Suhara, H. Tazaki, and H. Nishihara, Electron. Lett. **25,** 1326 (1989); R. W. Keys, A. Loni, and R. M. De La Rue, Electron. Lett. **26,** 624 (1990).
5. X. Cao, R. Srivastava, R. V. Ramaswamy, and J. Natour, IEEE Photon. Technol. Lett. **3,** 25 (1991).
6. N. Bloembergen and P. S. Pershan, Phys. Rev. **128,** 606 (1962).
7. M. L. Bortz and M. M. Fejer, Opt. Lett. **16,** 1844 (1991).
8. M. Lawrence and G. Edwards, Opt. Quantum Electron. **16,** 373 (1984).
9. E. J. Lim, M. M. Fejer, R. L. Byer, and W. J. Kozlovsky, Electron. Lett. **25,** 731 (1989).
10. F. Laurell, M. G. Roelofs, and H. Hsiung, Appl. Phys. Lett. **60,** 301 (1992).